Available online at www.sciencedirect.com
ScienceDirect
Trans. Nonferrous Met. Soc. China 19(2009) 1190−1195

Transactions of Nonferrous Metals Society of China
www.tnmsc.cn

High-temperature oxidation behavior of CeO_2-SiO_2/Ni-W-P composites

XU Rui-dong(徐瑞东)[1], WANG Jun-li(王军丽)[2], GUO Zhong-cheng(郭忠诚)[1], WANG Hua(王 华)[1]

1. Faculty of Metallurgy and Energy Engineering, Kunming University of Science and Technology,
Kunming 650093, China;
2. Research Center for Analysis and Measurement, Kunming University of Science and Technology,
Kunming 650093, China

Received 17 June 2008; accepted 16 June 2009

Abstract: Ni-W-P matrix composites containing CeO_2 and SiO_2 nano-particles were prepared on common carbon steel surface by means of pulse electrodeposition, and the high-temperature oxidation behavior was investigated. The results show that when the oxidation time is controlled in 1 h, oxidation kinetics curve between oxidation mass gain rate and oxidation temperature of CeO_2-SiO_2/Ni-W-P composites accords with the index increasing law. When the oxidation temperature is controlled at 300 ℃, the kinetics curve between oxidation mass gain rate and oxidation time accords with the linear increasing law. The composites as-deposited are in the amorphous state and turn into the crystal state at 400 ℃. The microstructures of oxidation film on the composites will change from the compact state to the loose state with increasing oxidation temperature to 800 ℃. They are still continuous and compact, and there are no crackle, strip and falling-out. CeO_2 and SiO_2 nano-particles co-deposited into Ni-W-P alloy can improve the high-temperature oxidation resistance.

Key words: pulse electrodeposition; metal matrix composites; nano-particles; high-temperature oxidation behavior

---

1 Introduction

In modern industries, mechanical products and parts should be able to run steadily for long term under high-temperature, high-pressure and high-speed conditions. Therefore, in order to improve the wear resistance, corrosion resistance and high-temperature oxidation resistance, surface strengthening technique is very important for increasing the service life and reliability, and improving the performance and quality of mechanical equipment.

Nano-particles reinforced metal matrix composites are made up of matrix metal and second phase particles that are dispersed evenly within the matrix metal, possessing comprehensive performance of the matrix metal and the second phase particles[1−3]. Compared with direct current electrodeposition, pulse electrodeposition with higher instantaneous current density is easy to prepare metal matrix composites with better performance by varying pulse parameters[4−5].

At present, co-deposition of some solid particles and matrix metal has been carried out[6−10], and there are also many reports about high-temperature oxidation behavior of Pd-Ni-Al coating and oxidation kinetics characterization of aluminized coating on Ni-base superalloy[11−12]. It was reported that the high-temperature oxidation resistance of RE-Ni-W-P-SiC composite material prepared by direct current electrodeposition is 3−4 times than that of Ni-W-P alloy [13]. CeO_2 and SiO_2 nano-particles imbedded into Ni-W-P matrix metal can improve microhardness, wear resistance and corrosion resistance[14]. However, the research on high-temperature oxidation behavior of this alloy has less been reported yet. In this work, CeO_2-SiO_2/Ni-W-P nano-particles reinforced metal matrix composites were prepared by pulse electrodeposition, and the high- temperature oxidation behavior was investigated. In the meantime, the phase structure and surface morphologies were also analyzed.

Foundation item: Project(20806035) supported by the National Natural Science Foundation of China; Project(2007E187M) supported by the Applied Basic Research Plans Program of Yunnan Province, China; Project supported by the Foundation for Leaders of Disciplines in Science and Technology of Yunnan Province, China; Project(08C0025) supported by the Scientific Research Fund of Yunnan Provincial Education Department, China; Project supported by the Training Foundation for Talents of Kunming University of Science and Technology, China

Corresponding author: WANG Jun-li; Tel: +86-13700619975; E-mail: rdxupaper@yahoo.com.cn

DOI: 10.1016/S1003-6326(08)60427-6

2 Experimental

2.1 Bath compositions and process conditions

The electrolyte compositions and processing parameters used to prepare CeO_2-SiO_2/Ni-W-P composites and Ni-W-P alloys are listed in Table 1.

Table 1 Electrolyte compositions and processing parameters used to prepare Ni-W-P/CeO_2-SiO_2 composites and Ni-W-P alloys

Item	CeO_2-SiO_2/Ni-W-P	Ni-W-P
$\rho(Ni_2SO_4 \cdot 6H_2O)/(g \cdot L^{-1})$	75	75
$\rho(C_6H_8O_7 \cdot H_2O)/(g \cdot L^{-1})$	120	120
$\rho(NaH_2PO_2 \cdot H_2O)/(g \cdot L^{-1})$	8	8
$\rho(Na_2WO_4 \cdot 2H_2O)/(g \cdot L^{-1})$	100	100
$\rho(CeO_2)/(g \cdot L^{-1})$ (Average size: 30 nm)	10	−
$\rho(SiO_2)/(g \cdot L^{-1})$ (Average size: 30 nm)	40	−
ρ(Surface active agent)/ $(mg \cdot L^{-1})$	6	−
pH value	6.5	6.5
Temperature/℃	60	60
Electrodeposition time/min	120	120
Mechanical stirring speed/ $(r \cdot min^{-1})$	1 000	1 000

Pulse parameters were as follows. Forward and reverse duty cycles were controlled at 10% and 30%; forward and reverse average current densities were 15 A/dm^2 and 1.5 A/dm^2; forward and reverse pulse working times were 300 ms and 40 ms, respectively. 316L stainless steel was used as anode material, and common carbon steel with dimensions of 30 mm×60 mm×2 mm was used as substrate material.

2.2 Process flow

To guarantee better dispersion of CeO_2 and SiO_2 nano-particles, before pulse electrodeposition, the electrolyte containing nano-particles was dispersed by ultrasonic with 400 W for 30 min. During the course of pulse electrodeposition, the mechanical stirring was used, and the stirring speed was controlled at 1 000 r/min.

The oxidizing process of samples was conducted in KSS−14XC box electric stove, and the heating rate was controlled at 10 ℃/min. Oxidation temperature was controlled at 100−800 ℃ and oxidation time was controlled in 1−5 h.

2.3 Analysis and measurement

EDS analysis was carried out on XL30 ESEM-TMP scanning electron microscope with phoenix spectrometer. The chemical compositions of the composites are Ni-9.89%W-8.59%P-7.35%CeO_2-2.81%SiO_2 (mass fraction); and the chemical compositions of the alloys are Ni-10.95%W-10.12%P (mass fraction). The mass of the samples before and after oxidation was measured by FA1004 electronic balance. The oxidation mass gain rate (the mass gain per unit oxidation area and oxidation time, g/(m^2·h)) was taken as the examination index. Phase structure of the samples was measured by D/Max2200 X-ray diffractometer, and the average size of Ni grains on the different crystal faces of (111), (220), (311) and (222) was calculated by means of MDI Jade software. Surface morphologies of the samples after oxidation were tested by XJZ−6 metallurgical microscope.

3 Results and discussion

3.1 Relationship between oxidation mass gain rate and oxidation temperature

When oxidation time is controlled in 1 h, oxidation kinetics curves between oxidation mass gain rate and oxidation temperature of CeO_2-SiO_2/Ni-W-P composites and Ni-W-P alloys are shown in Fig.1. Fig.1 displays that oxidation mass gain rate increases with the rise of oxidation temperature. When the oxidation temperature is lower than 400 ℃, the change of oxidation mass gain rate is little; but when the oxidation temperature is higher than 400℃, it increases comparatively obviously. At the same oxidation temperature, the oxidation mass gain rate of CeO_2-SiO_2/Ni-W-P composites is obviously lower than that of Ni-W-P alloys.

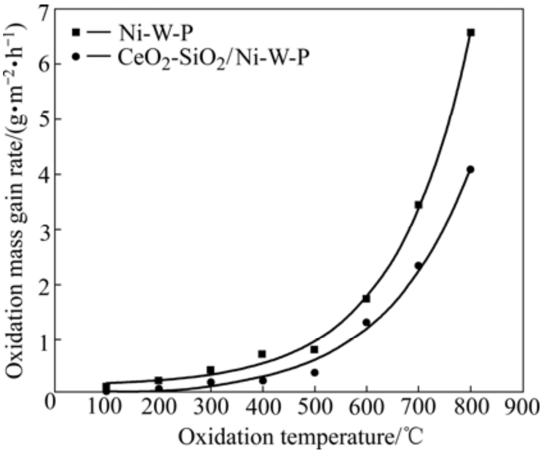

Fig.1 Oxidation kinetics curves between oxidation mass gain rate and oxidation temperature

According to the form of oxidation kinetics curves, the formula of $\Delta m=A+B\exp(T/C)$ is used as mathematics model, where Δm is oxidation mass gain rate; T is oxidation temperature; A, B and C are constants. Through nonlinear fitting for oxidation kinetics curves between oxidation mass gain rate and oxidation temperature, the oxidation kinetics equations and regression coefficient R can be obtained, as listed in Table 2.

It can be found out that the oxidation kinetics equations between oxidation mass gain rate and oxidation temperature accord with the index increasing law approximately, indicating that there is a certain index relationship between oxidation mass gain rate and oxidation temperature, namely, increasing oxidation temperature leads to the increase of oxidation mass gain rate according to the way of index increasing.

3.2 Relationship between oxidation mass gain rate and oxidation time

When the oxidation temperature is controlled at 300 ℃, oxidation kinetics curves between oxidation mass gain rate and oxidation time of CeO_2-SiO_2/Ni-W-P composites and Ni-W-P alloys are shown in Fig.2. Fig.2 shows that oxidation mass gain rate increases with the rise of oxidation time. At the same oxidation time, the oxidation mass gain rate of CeO_2-SiO_2/Ni-W-P composites is also obviously lower than that of Ni-W-P alloys.

According to the form of oxidation kinetics curves, the formula of $\Delta m=A+Bt$ is used as mathematics model, where Δm is oxidation mass gain rate; t is oxidation time; A and B are constants. Through linear fitting for oxidation kinetics curves between oxidation mass gain rate and oxidation time, the oxidation kinetics equations and regression coefficient R can be obtained, as listed in Table 3.

It can be known that the oxidation kinetics equations between oxidation mass gain rate and oxidation time accord with linear increasing law approximately, indicating that there is a certain linear relationship between oxidation mass gain rate and oxidation time, namely, increasing oxidation time leads to the linear increase of oxidation mass gain rate.

3.3 X-ray diffraction analysis

X-ray diffraction patterns of CeO_2-SiO_2/Ni-W-P composites as-deposited, oxidized at 400 ℃ and 600 ℃ are shown in Fig.3. It can be seen that the composites as-deposited are in the amorphous state and turn into crystal state when being oxidized at 400 ℃. At this time, the diffraction peak at 2θ=45° has differentiated obviously, and a great number of Ni_3P alloy phases, Ni_2P and N_5P_2 metastable phases precipitate from the matrix. When oxidation temperature is increased to 600℃, Ni_2P and N_5P_2 metastable phases have disappeared and changed

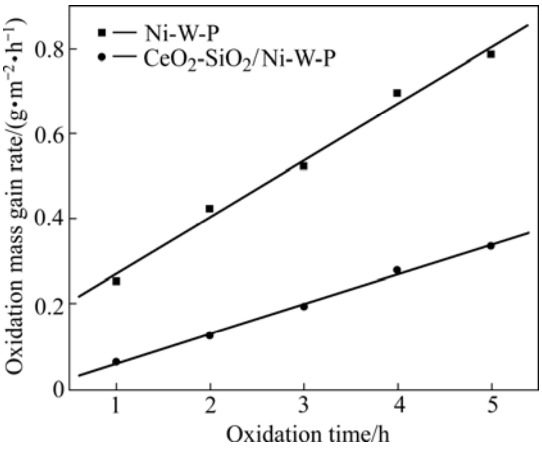

Fig.2 Oxidation kinetics curves between oxidation mass gain rate and oxidation time

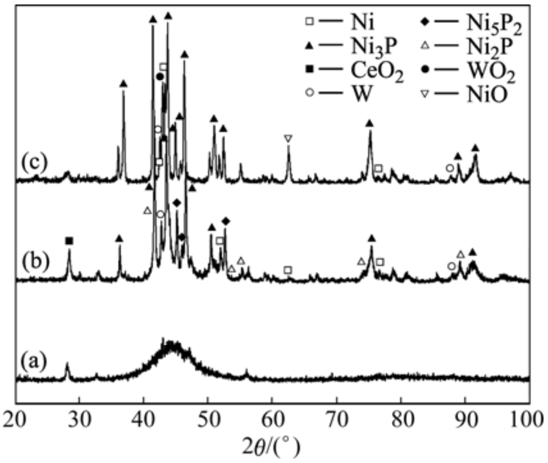

Fig.3 X-ray diffraction patterns of CeO_2.-SiO_2/Ni-W-P composites: (a) As-deposited; (b) 400 ℃; (c) 600 ℃

Table 2 Oxidation kinetics equations between oxidation mass gain rate and oxidation temperature and regression coefficients

Material	Oxidation kinetics equation	Regression coefficient, R	Range of oxidation temperature/℃
CeO_2.-SiO_2/Ni-W-P composites	Δm=−0.048 76+0.033 98exp(T/166.277 53)	0.993 50	100−800
Ni-W-P alloys	Δm=0.156 94+0.025 73exp(T/144.942 01)	0.998 08	100−800

Table 3 Oxidation kinetics equations between oxidation mass gain rate and oxidation time and regression coefficients

Material	Oxidation kinetics equation	Regression coefficient, R	Range of oxidation time/h
CeO_2.-SiO_2/Ni-W-P composites	Δm=−0.010 84+0.070 04t	0.998 18	1−5
Ni-W-P alloys	Δm=0.135 07+0.133 59t	0.995 12	1−5

into Ni_3P stable phases. The crystallinity increases further and the phase structure tends to be stable. Meanwhile, some Ni has already been oxidized as NiO and some W has been oxidized as WO_2. In addition, the diffraction peak of SiO_2 nano-particles cannot be found in the X-ray diffraction pattern owing to its amorphous structure.

3.4 Surface morphologies analysis

When oxidation time was controlled in 1 h, surface morphologies of CeO_2-SiO_2/Ni-W-P composites and Ni-W-P alloys at different oxidation temperatures are shown in Fig.4 and Fig.5, respectively. Fig.4 and Fig.5 display that with the increase of oxidation temperature and the aggravation of oxidation degree, the structure of

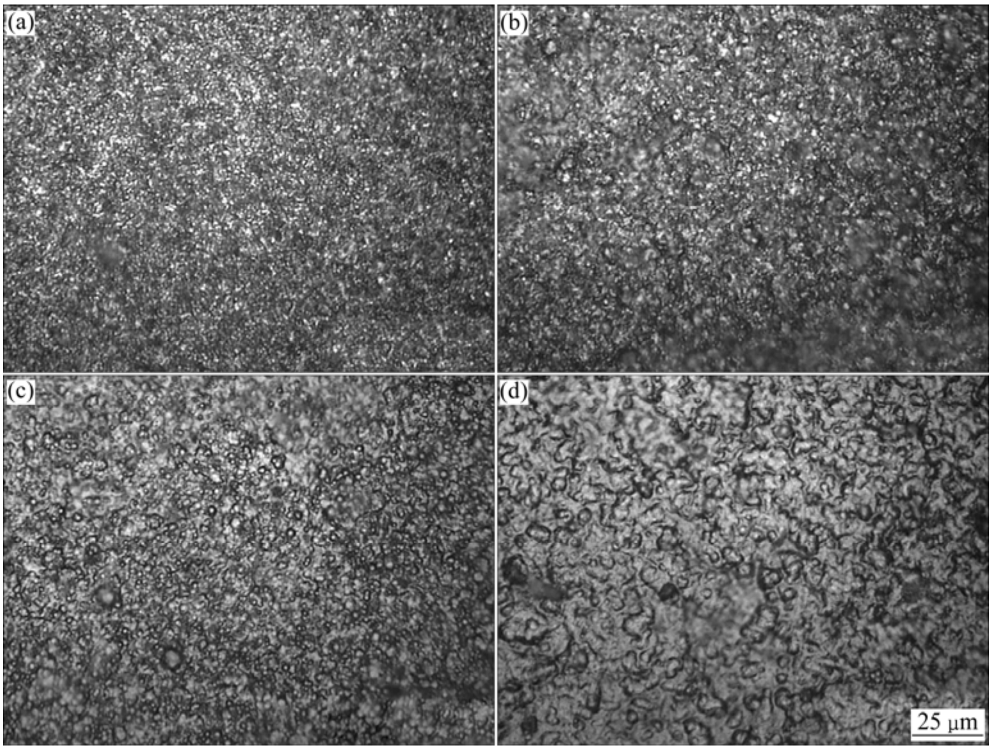

Fig.4 Surface morphologies of CeO_2-SiO_2/Ni-W-P composites under different oxidation temperatures: (a) 200 ℃; (b) 400 ℃; (c) 600 ℃; (d) 800 ℃

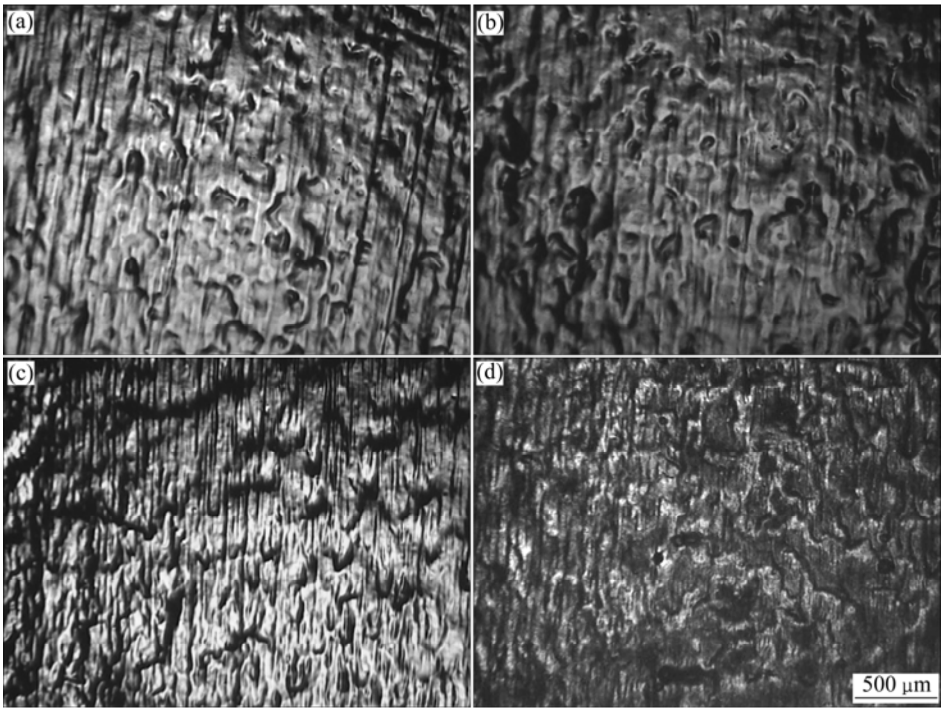

Fig.5 Surface morphologies of Ni-W-P alloys under different oxidation temperatures: (a) 200 ℃; (b) 400 ℃; (c) 600 ℃; (d) 800 ℃

the oxidation films changes from compact state to loose state gradually. When the oxidation temperature is improved to 800 ℃, the surface oxidation films of the composites are still intact, continuous and compact, and there are no crackle, strip and falling-out. However, those of Ni-W-P alloys are loose and porous; the oxidation particles are relatively big and a part has already turned into columnar crystal; even some pinhole and micro-crackle occur. Furthermore, it can be concluded tentatively that when the oxidation temperature is lower than 400 ℃, the change of surface morphologies is little. But after the composites and alloys have crystallized, the matrix metal grains begin to grow up in various degrees, which is particularly obvious at 600 ℃.

3.5 Grains growth analysis

As shown in Fig.3, it can be known that the composites have turned into crystal state when the oxidation temperature is increased to 400 ℃. In this moment, the average grain size of Ni grains on the different crystal faces of (111), (220), (311) and (222) can be calculated according to Scherrer formula by means of MDI Jade software, so as to judge the growth of grains during the oxidizing course.

The average grain size of Ni grains of CeO_2-SiO_2/Ni-W-P composites and Ni-W-P alloys are shown in Fig.6. Fig.6 displays that improving oxidation temperature leads to the increase of average grain size of Ni grains in various degrees. When the oxidation temperature is increased form 400 to 700 ℃, the average grain sizes of Ni grains of the composites and alloys are increased from 12.1 nm and 19.0 nm to 38.8 nm and 89.6 nm, respectively. It is obvious that increasing degree of average grain size of Ni grains for alloys is relatively large, indicating that CeO_2 and SiO_2 nano-particles co-deposited into Ni-W-P alloy can habit the growth of matrix metal grains, which is in agreement with surface morphologies analysis.

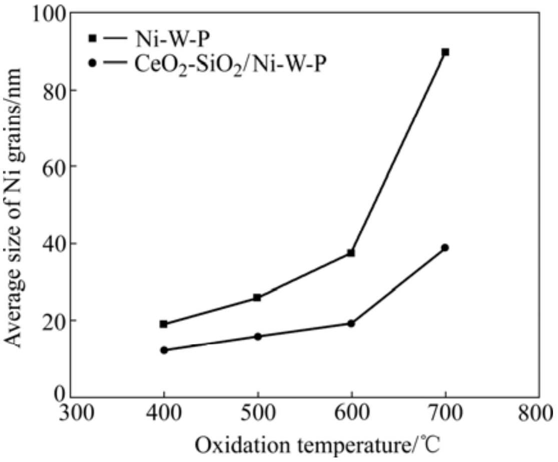

Fig.6 Relationship between average size of Ni grains and oxidation temperature

3.6 Oxidation mechanism

The above research shows that the high-temperature oxidation resistance of CeO_2-SiO_2/Ni-W-P composites is obviously better than that of Ni-W-P alloys. The main reason is as follows.

In as-deposited state, P atoms in Ni-W-P alloys are dissolved in Ni crystals and form supersaturated solid solution of Ni. With increasing the oxidation temperature, the atom diffusion aggravates and a large number of chemical compounds between Ni and P atom appear. Some chemical compounds are distributed within the materials and others are segregated in local area. These chemical compounds segregated in local area lead to the growth acceleration of Ni grains and serious oxidation. Meanwhile, it causes some structure defects and aggravates the oxidizing course of Ni-W-P alloys further.

The pulse co-deposition of CeO_2 and SiO_2 nano-particles with Ni-W-P matrix metal offers a large amount of forming core, inhabiting continuous growth of Ni-W-P matrix metal. So the structure of CeO_2-SiO_2/Ni-W-P composites is more intact, continuous and compact. It alleviates oxidizing process from surface to inside of oxidation films. When CeO_2 and SiO_2 nano-particles are imbedded in Ni-W-P matrix metal, a part is distributed on grain boundary defects, another part is packed by Ni-W-P matrix metal. During the course of oxidizing, these CeO_2 and SiO_2 nano-particles play a role of pinning, inhabiting growth of Ni grains and segregation of chemical compounds. Meanwhile, it causes chain reaction and makes Ni-P chemical compounds play such role as solid particles. In addition, the thermal stability of CeO_2 and SiO_2 nano-particles is very high, and their structure and shape do not change when oxidation temperature is lower 800℃, which can play mechanical shielding function and improve the high-temperature oxidation resistance of the composites.

4 Conclusions

1) The oxidation mass gain rate of CeO_2-SiO_2/Ni-W-P composites increases with increasing oxidation temperature or oxidation time. The oxidation kinetics curve accords with the equation: $\Delta m=-0.048\,76+0.033\,98\cdot\exp(T/166.277\,53)$ when the oxidation time is controlled in 1 h; while it accords with the equation: $\Delta m=-0.010\,84+0.070\,04t$ when the oxidation temperature is controlled at 300 ℃.

2) The composites as-deposited are in the amorphous state, and they turn into the crystal state at 400 ℃. The phase structure tends to be stable and some Ni_2P, N_5P_2 metastable phases change into Ni_3P stable phases at 600 ℃.

3) When the oxidation temperature is increased to 800 ℃, the oxidation films of the composites are still intact, continuous and compact, and there are no crackle, strip and falling-out. The co-deposition of CeO_2 and SiO_2 nano-particles into Ni-W-P matrix metal improves the high-temperature oxidation resistance of the composites.

References

[1] XU Rui-dong, WANG Jun-li, HE Li-fang, GUO Zhong-cheng. Study on the characteristics of Ni-W-P composite coatings containing nano-SiO_2 and nano-CeO_2 particles [J]. Surface and Coatings Technology, 2008, 202(8): 1574−1579.

[2] JIANG Bin, XU Bin-shi, DONG Shi-yun, WANG Hong-mei. Nano-power composite coatings [J]. Journal of Materials Protection, 2002, 35(6): 1−3. (in Chinese)

[3] ZHAO Xiao-bing, CHENG Zhi-gang. The Summary of nanocomposite and its preparation technology [J]. Journal of Jiangsu University: Natural Science, 2002, 23(4): 52−56. (in Chinese)

[4] DENNY T, RONNY L, ANDREAS B. Influence of pulse plating parameters on the electrocodeposition of matrix metal nanocomposites [J]. Electrochimica Acta, 2007, 52(25): 7362−7371.

[5] ZIMMERMAN A F, CLARK D G, AUST K T, ERB U. Pulse electrodeposition of Ni-SiC nanocomposite [J]. Materials Letters, 2002, 52(1/2): 85−90.

[6] SURENDER M, BALASUBRAMANIAM R, BASU B. Electrochemical behavior of electrodeposited Ni-WC composite coatings [J]. Surface and Coatings Technology, 2004, 187(1): 93−97.

[7] KIM S K, YOO H J. Formation of bilayer Ni-SiC composite coatings by electrodeposition [J]. Surface and Coatings Technology, 1998, 108/109(1/3): 564−569.

[8] BOGDAN S, MALGORZATA K. Composite Ni/Al_2O_3 coatings and their corrosion resistance [J]. Electrochimica Acta, 2005, 50(20): 4188−4195.

[9] WANG Li-ping, GAO Yan, XUE Qun-ji, LIU Hui-wen, XU Tao. Effects of nano-diamond particles on the structure and tribological property of Ni-matrix nanocomposite coatings [J]. Mater Sci Eng A, 2005, 390(1/2): 313−318.

[10] XU Rui-dong, GUO Zhong-cheng, WANG Jun-li. Study on Structure and properties of electrodeposited RE-Ni-W-B-B_4C-PTFE composite coating [J]. Trans Nonferrous Met Soc China, 2005, 15(3): 425−429.

[11] LI Meng-jin, SUN Xiao-feng, GUAN Heng-rong, JIANG Xiao-xia, HU Zhuang-qi. High temperature oxidation behavior of Pd-Ni-Al coating [J]. Acta Metallurgica Sinica, 2003, 39(7): 755−760. (in Chinese)

[12] WANG Yong-gui, QIU Er-ni, DING Ming-hui. Oxidation kinetics characterization of aluminized coating on Ni-base superalloy [J]. Hot Working Technology, 2007, 36(10): 48−50. (in Chinese)

[13] ZHU Xiao-yun, XU Rui-dong, GUO Zhong-cheng. Studies on high temperature oxidation of electrodeposited RE-Ni-W-P-SiC composite materials [J]. Transactions of Materials and Heat Treatment, 2004, 25(5): 1126−1129.

[14] XU Rui-dong, WANG Jun-li, GUO Zhong-cheng, WANG Hua. Effects of rare earth on microstructures and properties of Ni-W-P-CeO_2-SiO_2 nano-composite coatings [J]. Journal of Rare Earth, 2008, 26(4): 579−583.

(Edited by YANG Bing)